Wiley
Indoor Air
Volume 2025, Article ID 6684377, 10 pages
https://doi.org/10.1155/ina/6684377

WILEY

Research Article

Efficacy of Flow-Through Air Purification Device in Removing Aerosolized SARS-CoV-2

C. K. Law[1], **Joseph H. K. Lai**[1], **Roger G. N. Sze-To**[2], **R. S. Tuttle**[3], **K. Solocinski**[3], **J. E. Wilkinson**[3], **B. M. Cox**[3], **C. N. Huerter**[3] and **W. A. Sosna**[3]

[1]*Department of Building Environment and Energy Engineering, The Hong Kong Polytechnic University, Hong Kong, China*
[2]*Research and Development Department, Aurabeat Technology Limited, Hong Kong, China*
[3]*Translational Development, MRIGlobal, Kansas City, Missouri, USA*

Correspondence should be addressed to Joseph H. K. Lai; joseph.lai@polyu.edu.hk

Received 20 July 2023; Revised 13 August 2024; Accepted 4 February 2025

Academic Editor: Xiaohu Yang

The COVID-19 pandemic, attributed to the highly infectious nature of the SARS-CoV-2 virus, has prompted the exigent need for the development and evaluation of effective countermeasures. Previous studies have found that antimicrobial technology and increased ventilation can dilute virus concentration in the air or destroy SARS-CoV-2 on indoor surfaces, reducing the risk of spreading COVID-19. However, evidence showing the efficacy of air purifiers equipped with high-efficiency filters in the direct removal of aerosolized SARS-CoV-2 is limited. To plug this research gap, a study was pursued in which aerosolized virology testing was conducted to evaluate the efficacy of a flow-through air purification device in removing aerosolized SARS-CoV-2 (Delta variant). The device was equipped with an internal fan, a high-efficiency particulate air (HEPA) filter, UVC-LEDs, and an ionizer for multipass large-volume air recirculation. $TCID_{50}$ assays were conducted to quantify and compare the infectious SARS-CoV-2 with and without the operation of the device. It was found that the air purifier was highly effective in removing aerosolized SARS-CoV-2 virus, achieving over four-log reduction within 36 s of operation and under 10 equivalent air changes in the test chamber. These findings suggest that the tested air purifier is a useful countermeasure against the spread of COVID-19 in enclosed spaces. Further research is warranted to evaluate the efficacy of air purifiers in real-world indoor environments to ascertain the wider implications of using such purifiers in safeguarding public health against COVID-19.

Keywords: aerosol; air cleaning; COVID-19; Delta variants; SARS-CoV-2

1. Introduction

Since the first report of human-to-human SARS-CoV-2 transmission in December 2019, there have been over 664 million confirmed cases and 6.71 million deaths reported to the World Health Organization (WHO) [1]. This represents more than one-eighth of the global population infected with COVID-19, including over 36% of Europeans and 58% of Americans. Evidence from positive PCR results for SARS-CoV-2 in aerosol samples collected from quarantine and isolation facilities, hospitals, and residential settings, where infected individuals have stayed, suggests that SARS-CoV-2 has airborne transmission potential in addition to more direct contact and droplet transmission [2–6]. The WHO has also highlighted the existence of long-range aerosol transmission in poorly ventilated and/or crowded indoor settings [7].

SARS-CoV-2 genetic mutations play a significant role in the propagation of the virus. Studies have found that patients infected with SARS-CoV-2 variants such as Alpha, Delta, and Omicron may exhale more virus-laden aerosol than those infected with the wild type [8–10]. In addition to social distancing, universal masking, and vaccination, preemptive measures such as enhanced ventilation and air filtration are extensively deployed to lower the risk of COVID-19 exposure [11, 12]. Various researchers have identified that

the application of enhanced ventilation and air cleaners can reduce the age of air and the concentration of particulate matter (PM_{10}), suggesting a reduction in virus-laden aerosol in the air [13–15]. However, the removal of aerosol particles by increasing the ventilation rate may be limited by the capacity of pre-existing ventilation systems and may be insufficient to stop the rise in aerosol concentration [14].

Flow reactors utilizing UVC radiation and integrated systems designed for continuous air cleaning within heating, ventilation, and air conditioning (HVAC) systems, typically operating at a wavelength proximate to 254 nm, have demonstrated considerable efficacy in inactivating coronaviruses. A single pass through these systems can achieve a log10 reduction of active coronaviruses in excess of 2.2 when operating at a flow rate of 146 m^3/h and subject to a UVC dose of 13.9 mJ/cm^2 [16]. This efficacy is further amplified at decreased flow rates, with log10 reduction exceeding 3.7 (corresponding to a removal efficiency of 99.98%) at a flow rate of 41 m^3/h, under an elevated UVC dose of 49.6 mJ/cm^2 [16]. The effectiveness of UVC irradiation is not restricted to the 254 nm wavelength. Irradiation peaking at 222 nm, at doses of 23 mJ/cm^2, has been shown to achieve reductions of viable SARS-CoV-2 by 92% [17]. The use of ultraviolet C light-emitting diodes (UVC-LEDs) with simple electricity, fast stabilizing intensity, and insensitivity to temperature widened the application in different devices [18, 19]. These findings reinforce the potential of UVC radiation as a tool for curtailing the spread of SARS-CoV-2 and other coronaviruses. Compared to standalone air cleaners placed in specific indoor locations, flow reactors with UVC radiation offer more controlled UVC radiation exposure, potentially enhancing inactivation efficiency but limited by the duration of air exposure to the UVC source.

Researchers have used computational fluid dynamics (CFDs) to simulate the filtration effectiveness of portable air cleaners [20–24], and real measurements have been carried out to identify that air cleaners can remove aerosol particles from indoor settings [25, 26]. In addition to air filtration, different physical mechanisms (e.g., heating, plasma, and laser) have been identified as useful for inactivating aerosolized SARS-CoV-2. For instance, exposure of aerosolized SARS-CoV-2 to a temperature of 150°C or 220°C can result in a 99.9% or 99.999% reduction in viability, respectively [27]. Airflow containing SARS-CoV-2 passed through a dielectric filter discharge has more than 99.84% inactivation with degradation of SARS-CoV-2 genes [28]. Furthermore, a device emitting 10,600 nm laser light can inactivate over 99% of SARS-CoV-2 in the air in less than 15 ms [29]. However, the extant literature does not provide comprehensive findings on the effectiveness of modern air purification devices specifically against SARS-CoV-2 variants associated with aerosols generated from critical settings. To bridge this research gap, the present study was conducted to provide empirical evidence of an air cleaner (equipped with a HEPA filter, UVC-LEDs, and an ionizer for multipass large volume air recirculation) in removing airborne viruses in localized scenarios, particularly with the high viral load within the small chamber.

2. Method

2.1. Flow-Through Air Purification Device. The air purification device used in this study was Model NSP-W1 of Aurabeat, which was equipped with a 40 mm HEPA filter (Manufacturer: Aurabeat, Grade: H13) that can remove over 99.97% of particles down to 0.3 μm [30]. The device has dimensions of 600 × 213 × 437 mm and was delivered with a 110 V power supply. At its highest fan speed setting, the device can provide a clean air delivery rate (particle-free) of approximately 370 m^3/h, in accordance with the GB/T 18801-2015 test protocol for air cleaners, which utilizes a "pull-down approach" by accumulating a high particle concentration (particle $\geq$0.3 μm, 2×10^6–2×10^7 pcs/L) in a 30 m^3 test chamber before running the device at maximum airflow for 1 h. Air is drawn in through the air intake located at the perimeter of the front cover and is distributed from the top outlet (see Figure 1). The device features an internal fan that drives the air to pass through the HEPA filter before outputting the filtered air through the top of the unit. Additional features, including UVC-LEDs and an ionizer, are equipped in the device to aid its efficacy. Two UVC-LEDs are independently positioned 130 mm beneath the center of the suction inlet, while the ionizer is situated 20 mm below the right air outlet. During the test, the device was placed in the center of the test chamber. The device was operated for 36 s during the test, which, given the chamber volume of 0.37 m^3, is equivalent to approximately 10 air changes.

2.2. Test Design. To evaluate the efficacy of the flow-through air purification device in removing aerosolized SARS-CoV-2 from the test environment, investigations were conducted in three independent replicates for both the control and device tests. The control test was conducted in triplicate to measure the natural aerosol concentration characteristics in the chamber without the operation of the device, which was placed in the center of the test system. For the device test, the device was operated at its highest fan speed setting using the same viral stock suspension, aerosol generation, system operation conditions, and sampling intervals as the control test. The results obtained from the control test provided a standard against which to compare the efficacy of the device in removing airborne SARS-CoV-2 from the air.

2.3. Virus and Cell. The SARS-CoV-2 lineage B.1.617.2 (Delta variant) used in this study was obtained from BEI Resources (NR-55611) and was isolated in Memphis, Tennessee, United States. The virus strain was propagated in TMPRSS-2 Vero E6 cells obtained from BPS Bioscience Inc. (Genbank#: NM_005656.4, Passage No.:17) [31]. The cells were cultured in growth media; this media consisted of Dulbecco's modified Eagle medium/F12, supplemented with 5% fetal bovine serum (FBS) and G418 sulfate [32]. Cells were infected with the virus at approximately 80% confluency, and the supernatant was harvested once approximately 80% cell death due to cytopathic effects (CPEs) was observed. This usually occurs 2–3 days after infection. The supernatant was centrifuged to pellet cell debris, aliquoted, and frozen at −80°C until use. Cells used for $TCID_{50}$

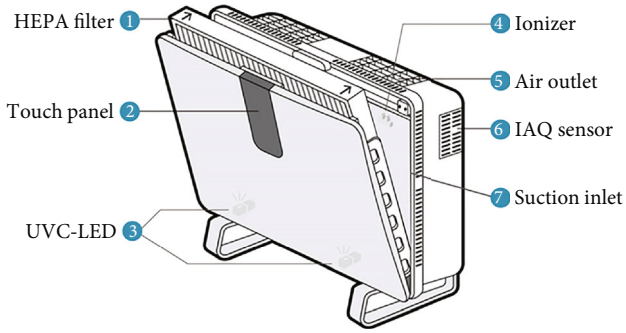

FIGURE 1: Composition of the flow-through air purification device.

experiments were plated so as to be 80%–100% confluent on the day of testing and inoculation [33].

2.4. Aerosol Generation System. To carry out the aerosolized infectious viral test in a safe and controlled manner, a Plexiglas-fabricated chamber was constructed inside a Class III Biosafety Cabinet. The detailed specifications, dimensions, and associated equipment are presented in Figure 2. The test setup includes an aerosol containment chamber, an aerosol generation system, a test device, a sampler, and associated digital flow controllers and meters to ensure accurate measurements and control of the experimental conditions.

For the aerosolized infectious viral test, the SARS-CoV-2 virus with a titer of 1.47×10^7 $TCID_{50}$/mL was aerosolized using a Collison 6-jet nebulizer into the enclosed test chamber for 15 min. DMEM/F12 was also used in the SARS-CoV-2 virus suspension that was added to the nebulizer for aerosolization. The selection of DMEM/F12 as the suspension medium is critical for maintaining the viability of the SARS-CoV-2 virus [34]. DMEM/F12 provides a stable nutrient environment that preserves viral viability throughout various stages, including storage, preparation, testing, sampling, and concentration analysis [35]. This stability is essential for the accurate assessment of the test device's performance, as it prevents the decay of viral stock and sample concentration due to environmental effects that would typically occur with water or other non-nutrient media [36]. The nebulizer received clean air supplied by an air tank at a pressure of 26 psi (179 kPa) and a flow rate of 15 L/min (0.9 m^3/h). To ensure the air supply was particle-free for aerosol sampling, a dual HEPA capsule filter was installed upstream of the nebulizer. The chamber fan was continuously operated to achieve uniform mixing and a homogeneous concentration of aerosols within the test system during aerosol generation and the sampling period.

2.5. Aerosol Collection and Sampling. To collect aerosol samples, an impinger sampler, specifically an AGI-30 impinger model 7540 (Ace Glass Inc.) filled with 20 mL of DMEM/F12, was utilized. The impinger sampler was operated at a flow rate of 0.75 m^3/h and collected aerosols from the test chamber into sterile conical tubes. The collected samples were then transferred to a secondary container and transported to another BSL-3 laboratory for inoculation and recovery of the virus on the test sample.

Aerosol analysis was performed for each control and device test using a TSI Aerodynamic Particle Sizer (APS) 3321 spectrometer, which can measure the dynamic particle measurement range of 0.3–20 μm. The APS provides real-time measurements of mass median aerodynamic diameter (MMAD), geometric standard deviation (GSD), total sample aerosol mass (milligrams per cubic meter), and aerosol particle counts (#/m^3). The APS was programmed to take sequential 10-s aerosol scans over the course of the test, with sampling conducted both prior to and after device operation (see Figure 3). Before the device test, three sequential samples were taken to establish natural aerosol decay results and ensure consistency and reproducibility of aerosol challenge concentrations and particle size characteristics for all control and device tests. Starting from device operation, APS particle counts were taken sequentially over the test period of 20 min.

2.6. Inoculation and Recovery of the Virus. Viral aerosol samples were collected using a sterile AGI-30 impinger model 7540 (Ace Glass Inc.) filled with 20 mL of DMEM/F12 for each test. Impinger samples were transferred to a Class II Biological Safety Cabinet to perform the $TCID_{50}$ assay. The impinger samples were serially diluted 1:10 down a 24-well plate of cells in DMEM/F12 to assess the $TCID_{50}$ of the samples. Following a 15-min incubation period to allow the virus to adsorb to cells without interference from FBS, DMEM/F12 supplemented with 5% FBS was added to the cells to feed them for the next 5 days, allowing for viable viral analysis.

2.7. Removing Efficacy of the Air Purification Device. After the test, the 24-well plates were examined using a microscope for the presence of CPE associated with viral presence and replication 5 days after inoculation. Any well-displaying CPE, which is often characterized by detachment from the plate, round shape, less transparency, and smaller size than living cells, was marked as either the whole well-being affected or only a small patch, as both are indicative of the presence of a viable virus.

The numbers of positive and negative wells were recorded and entered into a modified spreadsheet published by Lindenbach [37]. The $TCID_{50}$/mL was calculated using the following equations:

$$PD = \frac{CPE_{(n,>50\%)} - CPE_{(n,50\%)}}{CPE_{(n+1,>50\%)} - CPE_{(n+1,<50\%)}} \quad (1)$$

where PD is the proportionate distance between the two dilution levels, $CPE_{(n,>50\%)}$ is the percent CPE at the dilution level n just above the 50% threshold, $CPE_{(n,50\%)}$ is the percent CPE at the dilution level n just the 50% threshold, $CPE_{(n+1,>50\%)}$ is the percent CPE at the next dilution level $n+$

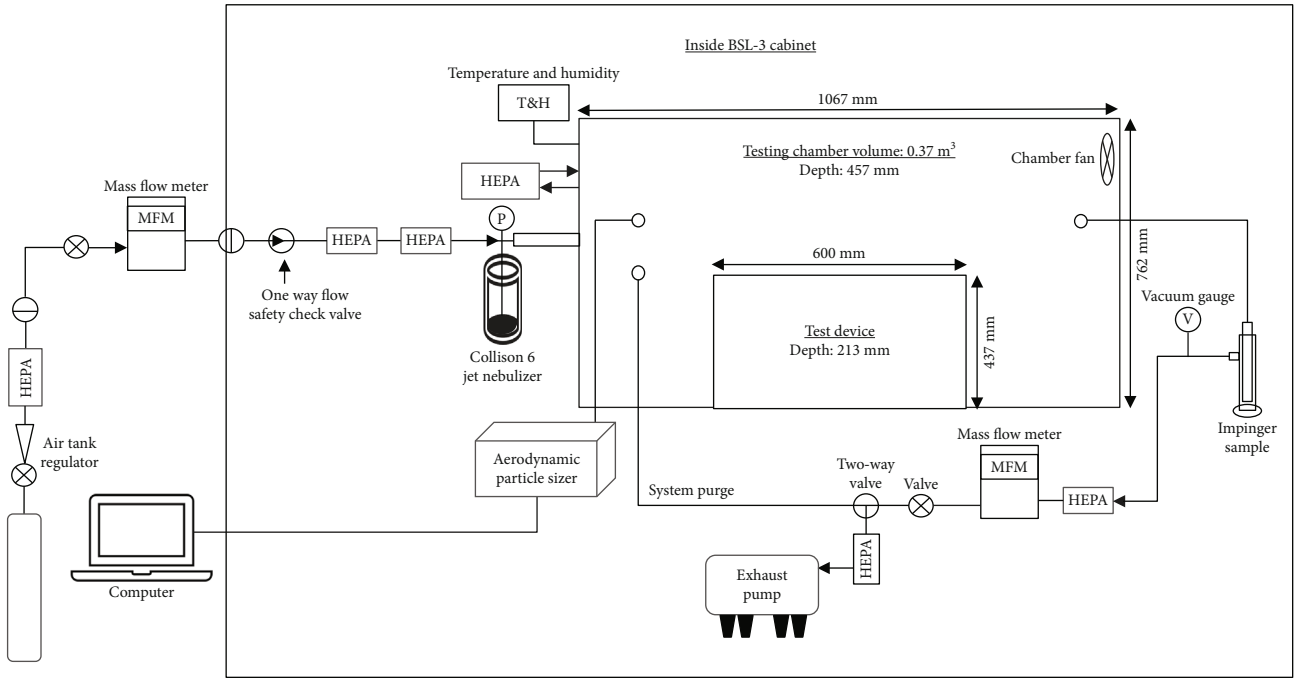

Figure 2: SARS-CoV-2 aerosol test system.

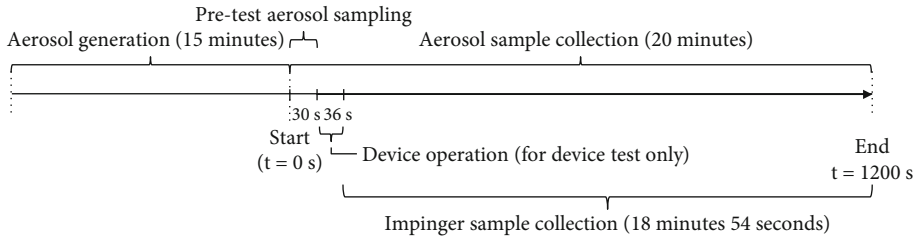

Figure 3: Aerosol sampling timeline.

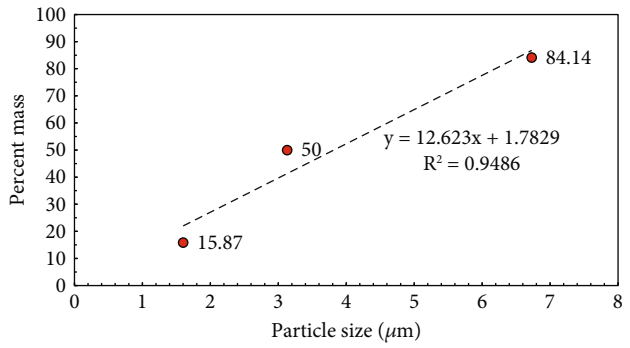

Figure 4: Aerosol particle size distribution.

1 above the 50% threshold, and $CPE_{(n+1,<50\%)}$ is the percent CPE at the next dilution level $n + 1$ below the 50% threshold.

$$TCID_{50} = 10^{\log \text{ of dilution above } 50\%CPE} - PD \quad (2)$$

where $TCID_{50}$ is the dilution level at which 50% of the cell cultures are infected, which is a common measure of viral infectivity.

$$TCID_{50}/mL = \frac{1}{V_{well} \times TCID_{50}} \quad (3)$$

where $TCID_{50}$/mL is the concentration of the virus that results in a 50% CPE per milliliter, which is a common measure of viral infectivity, and V_{well} is the volume (in milliliters) used for each well in the cell culture plate.

The log10 of the three technical replicates was averaged for control and treatment samples. This number for the treatment is subtracted from the number for the control and is reported as "log reduction." This log reduction is converted into a percent log reduction via the following equation.

$$\%\text{Log reduction} = \left(1 - 10^{-\log \text{ reduction}}\right) \times 100 \quad (4)$$

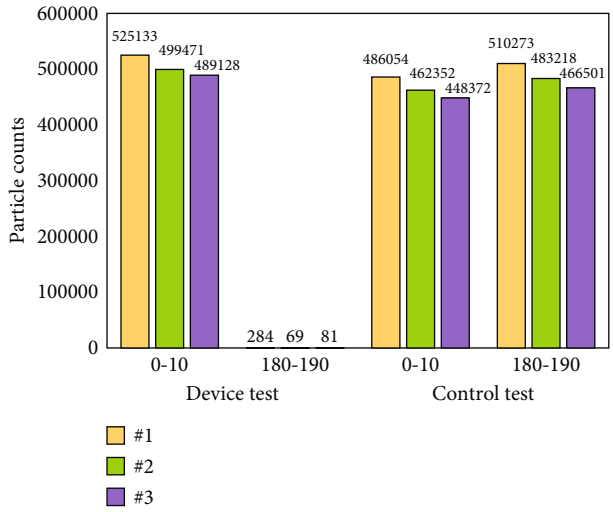

Figure 5: Particle counts in the device and control tests.

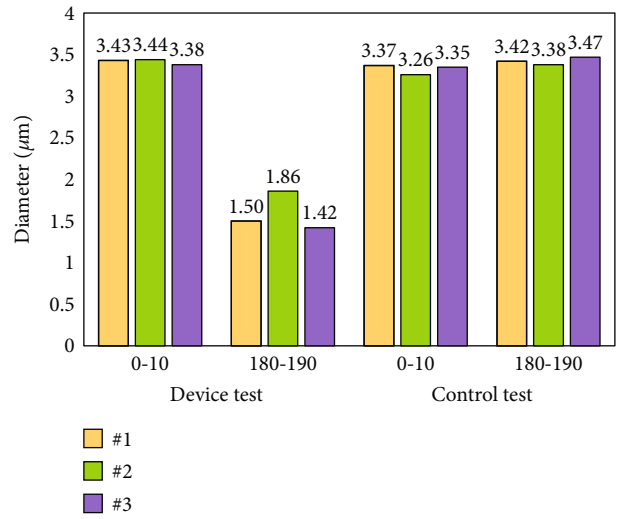

Figure 7: Particle diameter in the device and control tests.

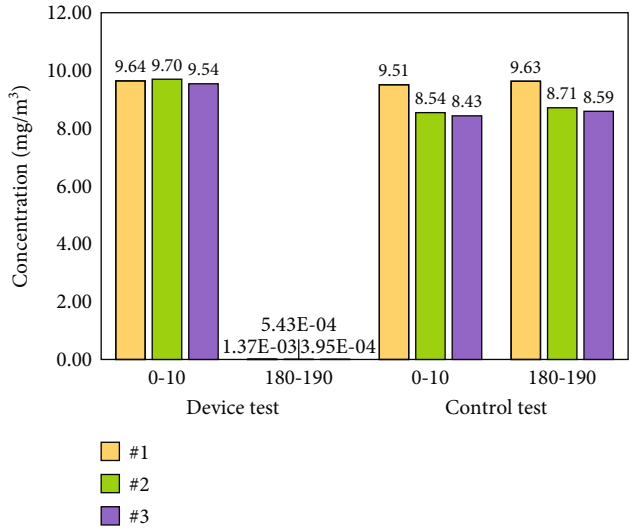

Figure 6: Particle concentration in the device and control tests.

where %Log reduction is the percentage reduction in the concentration of the virus.

3. Results and Discussion

3.1. Aerosol Characteristics. The percent mass of the SARS-CoV-2 aerosol particle size distribution from a representative APS sample is plotted in Figure 4. The graph shows the particle size on the x-axis and the percent aerosol mass on the y-axis. The MMAD reflects a median diameter of approximately 3.13 μm, with 50% of the aerosol particle mass below and 50% above the median diameter. The 15.87% mass (1.60 μm) and 84.14% (6.73 μm) particle mass points with associated particle size are also indicated. The 15.87% and 84.14% mass size diameters are used in the plot to define the linear regression fit of the data as shown on the graph and the GSD of the size distribution. The GSD is computed as the ratio $d84.14/d50 = d50/d15.87$ for unimodal aerosol particle size distributions. The data shows the span from d84 to d50 and from d50 to d84 percent mass particle sizes of the distribution to be proportional and reflective of a unimodal aerosol size distribution. These results are consistent with those reported for virus-laden aerosol particle sizes, with more than 90% of exhaled SARS-CoV-2 RNA found in aerosol particles < 4.5 μm, and the highest concentrations found in 0.94–2.8 μm particles [38]. Other studies have also found that both fine (≤ 2.5 μm) particle-associated SARS-CoV-2 and coarse (2.5–10 μm) virus-laden particles can be found in COVID-19 patient rooms [39].

The APS count, concentration, mass, and mass median particle sizes obtained from the control and device tests were analyzed. Data recorded from $t = 0$ to 10 s and from $t = 180$ to 190 s, representing the aerosol characteristics before and after device operation, are compared in Figures 5, 6, and 7 and Table 1.

The particle count in each device test (T1–T3) demonstrated an impressive reduction of over 99.9% (Figure 5), while particle concentration from T2 to T3 exhibited reductions of up to 99.99% (Figure 6). Additionally, particle diameter experienced a significant decrease ranging from 46% to 58% across the tests (Figure 7). In the control test, however, notable dynamics were observed, with particle count and particle concentration increasing by 4.04% and 1.26%, respectively, alongside a slight rise in particle diameter from 1.48% to 3.68% (Figure 7). These changes suggest mechanisms such as resuspension or aggregation, likely driven by turbulence or imperfect mixing within the chamber, which can inhibit settling and induce fluctuations in particle distribution. While measurement variability is acknowledged, the consistent trends across multiple parameters highlight the necessity for further investigation to elucidate the complex dynamics influencing particle behavior in closed systems.

Table 1: Aerosol characterization recorded in the control and device tests.

Test no.[a]	Time (seconds)	Average particle counts	Average concentration (mg/m^3)	Average diameter (μm)
T1–T3	0–10	504,577	9.63	3.42
T1–T3	180–190	145	8×10^{-4}	1.59
Cl–C3	0–10	465,593	8.63	3.33
Cl–C3	180–190	486,664	8.98	3.42

[a]"T" denotes device test; "C" denotes control (without any device operation).

In the initial 10-s interval, both test scenarios (T1–T3 and Cl–C3) exhibit remarkably high average particle counts: 504,577 and 465,593, respectively, reflecting a difference of less than 10% (Table 1). In contrast, the data recorded in the interval of 180–190 s reveal a dramatic decrease in the average particle count for T1–T3, plummeting to 145. This substantial reduction, coupled with a corresponding decrease in average concentration to 8×10^{-4} mg/m^3, shows that effective removal mechanisms existed. Conversely, the Cl–C3 test results demonstrate a more stable particle presence during the same period. The average diameter of particles in this interval for the Tl–T3 scenarios was recorded at 1.59 μm, indicating that small particles with low concentrations persisted opportunistically in the air.

The particle counts profile for both the control and device tests is presented in Figure 8, with data averaged from three independently replicated tests. The baseline reference was obtained from the control test to measure the natural aerosol decay. The particle counts recorded in the control tests remained relatively constant with an insignificant decline, while the particle counts recorded in device tests showed a rapid decay. The particle counts were reduced to less than 100 after the device had operated for 36 s. The reading of particle counts fluctuated between 49 and 94 after the device was turned off.

The particle counts recorded after the deactivation of the device exhibited a downward trend (Figure 8). By the end of the measurement period, the particle count did not reach zero, a finding that aligns with previous studies [40, 41]. Examining in detail the pattern of significant drops in the particle counts during the first 60 s postactivation period (t = 30–90 s) found that (i) the decay curve exhibits an exponential fit (Figure 9) and (ii) the downward trend of the particle counts (in natural log values) largely follows a linear pattern (Figure 10). The coefficients of determination (R^2) of both of these fits exceed 0.9.

The viability of the virus in each sample is shown in Figure 11, where the $TCID_{50}$/mL of virus stock is 1.47×10^7 and the Log_{10} $TCID_{50}$/mL value is 7.17. The findings show a significant viral removal across the various test samples when compared to the control. Specifically, the average $TCID_{50}$/mL for the test scenarios was recorded at 0.372, in contrast to the control value of 4480. Furthermore, Figure 12 illustrates a comparative analysis between the test and the control for each sample: the logarithmic values of TCID50/mL for both the test and control scenarios provide a clear understanding of the percentage reduction in viral concentration. Using Equation (4), the percentage reductions of the virus of the three tests range from 99.990% to 99.993%, with an average reduction of 99.992%.

3.2. Implication and Future Work. Air purification devices may integrate various antiviral technologies and mechanisms, such as UVC, ionization, plasma, and antimicrobial coating. In this context, a multifunctional air purification device featuring HEPA filter, two UVC-LEDs (each rated power: 0.4 wattage, intensity at 15 cm: 15.2 μW/cm^2), and a negative ionizer (rated power: 0.85 wattage, ion concentration 200 mm away from the device: 5×10^6 pcs/cm^3) was deployed in a chamber measuring 0.37 m^3 to investigate the removal of airborne SARS-CoV-2 variants. As shown above, the air purification device, operating at its maximum speed of 370 m^3/h (equating to 6166.67 L/min), successfully eliminated over 99.992% of the airborne SARS-CoV-2 variants within 36 s. By applying the principle of conditional probability in analyzing the virus reduction at each air change rate, the airborne reduction rate was calculated as 61.07%, 84.84%, and 99.87% at 1, 2, and 7.1 air changes, respectively.

These findings can be compared with those from previous research [42], which assessed the efficacy of an air purification device that was equipped with a HEPA filter. That device operated at a low-flow condition (48 L/min) for several minutes (5, 10, and 35.5) in a smaller 0.24 m^3 chamber. The test outcomes showed that the airborne virus was reduced by 85.38%, 96.03%, and 99.97% at 1, 2, and 7.1 ventilation volumes, respectively.

The difference in the relationship between the air change rate and remaining virus in the chamber between our study and the previous research may be due to differences in the operational conditions, device characteristics, and chamber geometry. Additionally, our device's inclusion of UVC-LEDs and ionizers, which were not equipped in the device used by Lindenbach et al. [37], may also be a contributing factor. Future studies are recommended to investigate the effects of these factors in order to add knowledge to this field.

On-site empirical studies should also be conducted in real-world indoor environments to prove the efficacy of air purification devices. In particular, elevators and other confined spaces with a high occupant density may pose a higher risk of airborne particle exposure for the users, especially when there are infected persons coughing or sneezing in the space [43]. The flow dynamics of existing ventilation

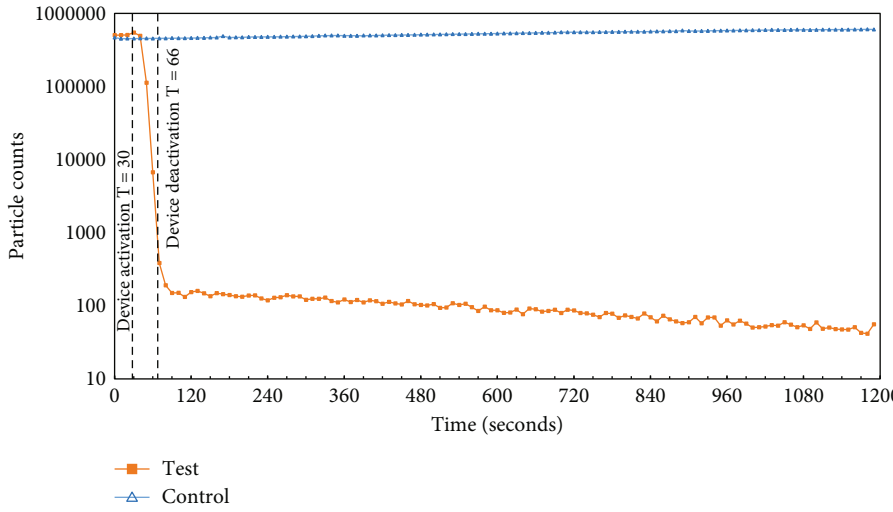

Figure 8: Particle count profile during the control and device tests.

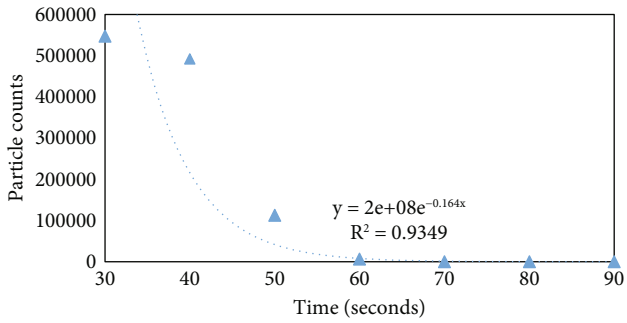

Figure 9: Decay pattern of particle counts.

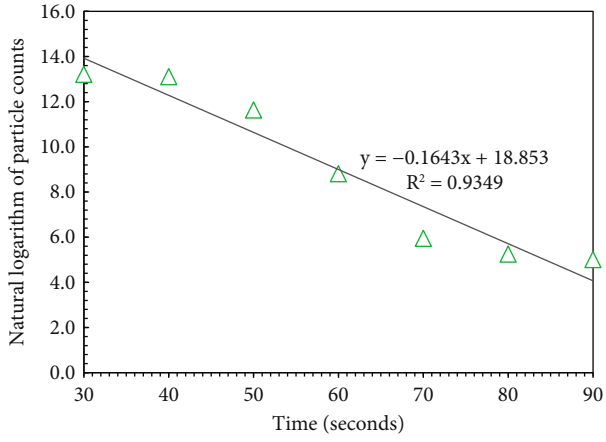

Figure 10: Decline pattern of particle counts (natural log).

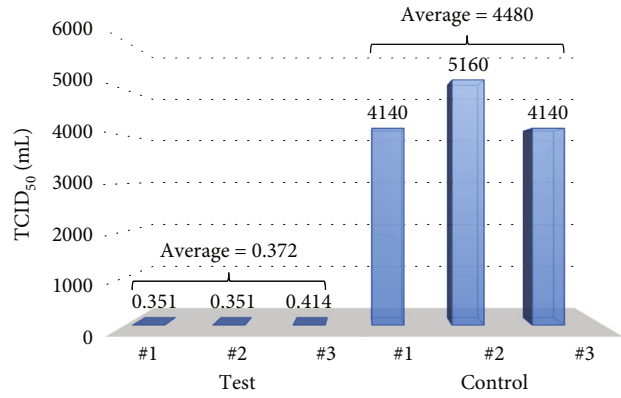

Figure 11: $TCID_{50}$/mL acquired for test and control.

systems may also affect the actual performance of the air purification device [44]. Using some harmless surrogate virus on-site may be a more practical approach to testing, considering the potential danger of using high-risk airborne viruses. During device testing and operation, the relationship between the mass loaded onto the air filter and its flow rate should be investigated to avoid filter aging in the test and performance drop in long-term operation.

Alternatively, an extensive survey can be conducted to compare COVID-19 incidence indoors with and without air purifiers. The Centers for Disease Control and Prevention (CDC) has found that filtration methods are associated with lower COVID-19 incidence in schools [45]. When schools applied dilution methods alone, the COVID-19 incidence was 35% lower than the base with no ventilation strategy implemented. Both dilution and filtration methods applied simultaneously can bring a 48% lower incidence of COVID-19. However, the study did not explore filtration alone, air change provided by natural ventilation, and how these two factors contribute to a lower incidence of COVID-19. Of note, commercial buildings, residential buildings, and even hospitals have different characteristics compared to school environments, and the pressurization of different zones, demand control logics, fresh air supply, and so on may complicate the study and require future exploration in relation to case incidence.

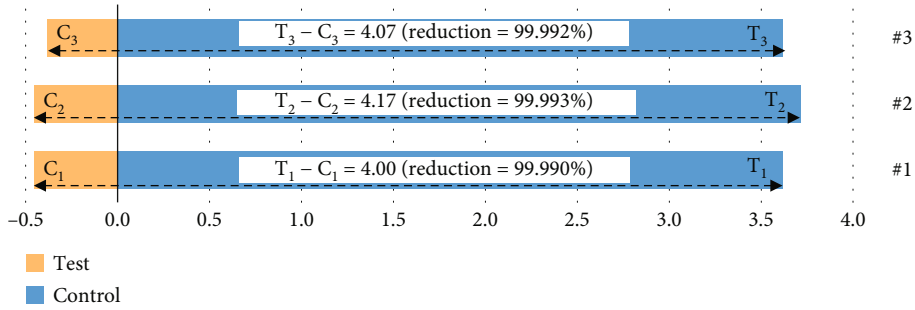

Figure 12: Log reduction and percentage reduction for test and control.

4. Conclusions

Our study demonstrates the efficacy of a flow-through air purification device that utilizes a HEPA filter, with ionizer and UVC-LEDs, in removing aerosolized SARS-CoV-2 virus (Delta variant) from a test chamber containing high concentrations of airborne viruses. Under the experimental conditions, the device was able to remove more than 99.992% of aerosolized SARS-CoV-2 within 36 s of operation, producing approximately 10 air changes during the test, as compared to the control test results with the device not in operation.

This research provides a foundation for further investigation into the relationship between air change, test space, and virus reductions. To our knowledge, it is the first study that evaluates the efficacy of a flow-through device with a HEPA filter, an ionizer, and UVC-LEDs in removing the aerosolized SARS-CoV-2 Delta variant. The limited research on air purifier performance against this specific variant makes our findings particularly significant.

While the acute phase of the COVID-19 pandemic is over, recently there are signs alerting the need to guard against the virus and its variants; in July 2024, for instance, a 39% week-on-week surge in infections occurred in Japan [46]. Therefore, the preparedness for the next public health emergency of this kind remains essential. Engineering interventions, such as the strategic use of air purification devices, emerge as a prudent and cost-effective mitigation strategy when juxtaposed with alternatives like vaccine development that demand prolonged validation and risk mitigation processes. This study also exemplifies a rigorous challenge testing methodology tailored to assess the efficacy of air purification devices within environments teeming with highly infectious viruses, thereby furnishing building owners, operators, and occupants with invaluable insights for fortifying indoor environments against a spectrum of diseases. By showcasing the efficacy of a modern air purification device in high-risk settings, this research underscores the pivotal role of engineering solutions in bolstering indoor air quality and fortifying defenses against pathogenic intrusions, thereby setting a new standard for future indoor environmental health considerations.

Admittedly, the study reported above is not free from limitations. Considering the size of the test chamber, further empirical studies are recommended to confirm the effectiveness of the air purification device in larger, real-world indoor environments, especially for confined spaces (e.g., elevators) posing high airborne particle exposure to occupants. Factors such as air movement induced by HVAC systems and the presence of occupants also warrant due consideration. As the focus of this study was not on the effectiveness of the individual components (filters, ionizers, and UVC-LEDs) in virus removal, future research should examine their effectiveness in different combinations. Worth exploring, too, are design improvements of the air purification device. They include the deployment of high-efficiency brushless motors to enhance airflow, modification of the mold design to increase the air inlet area and prevent air short-circuiting, and an increase in the number and power of UVC-LEDs to augment supplementary virus reduction.

Data Availability Statement

Raw data is available on request from the corresponding authors.

Disclosure

The opinions expressed in this publication are those of the authors and do not reflect the opinions of MRIGlobal.

Conflicts of Interest

Except for one of the authors who is affiliated with Aurabeat Technology Limited, which provided financial support for the experiments conducted in this research, the authors declare that they have no known competing financial interests or personal relationships that could have potentially influenced the work reported in this paper.

Author Contributions

C.K.L.: investigation, writing original draft, and visualization. J.H.K.L.: writing (review and editing). R.G.N.S.-T.: writing (review and editing). R.S.T.: methodology, test system design, validation, and writing (review and editing). K.S.: methodology, validation, and writing (review and editing). J.E.W.: methodology, validation, and writing (review and editing). B.M.C.: methodology, validation, and writing (review and editing). C.N.H.: methodology, validation, and writing (review and editing). W.A.S.: review, editing, and project management.

Funding

The experiment was financially supported by the Research and Development Department of Aurabeat Technology Limited.

Acknowledgments

The authors would like to express their gratitude to Aurabeat Technology Limited for providing financial support for the experiments conducted by MRIGlobal.

References

[1] WHO, "WHO coronavirus (COVID-19) dashboard," 2023, Accessed June 2023, https://covid19.who.int/.

[2] Y. Liu, Z. Ning, Y. Chen et al., "Aerodynamic analysis of SARS-CoV-2 in two Wuhan hospitals," *Nature*, vol. 582, no. 7813, pp. 557–560, 2020.

[3] J. L. Santarpia, D. N. Rivera, V. L. Herrera et al., "Aerosol and surface contamination of SARS-CoV-2 observed in quarantine and isolation care," *Scientific Reports*, vol. 10, no. 1, Article ID 12732, 2020.

[4] G. Correia, L. Rodrigues, M. Afonso et al., "SARS-CoV-2 air and surface contamination in residential settings," *Scientific Reports*, vol. 12, no. 1, Article ID 18058, 2022.

[5] N. Rufino de Sousa, L. Steponaviciute, L. Margerie et al., "Detection and isolation of airborne SARS-CoV-2 in a hospital setting," *Indoor Air*, vol. 32, no. 3, Article ID e13023, 2022.

[6] T. Greenhalgh, J. L. Jimenez, K. A. Prather, Z. Tufekci, D. Fisman, and R. Schooley, "Ten scientific reasons in support of airborne transmission of SARS-CoV-2," *The Lancet*, vol. 397, no. 10285, pp. 1603–1605, 2021.

[7] WHO, "Coronavirus disease (COVID-19): how is it transmitted?," 2021, Accessed June 2023, https://www.who.int/news-room/questions-and-answers/item/coronavirus-disease-covid-19-how-is-it-transmitted.

[8] J. R. Port, C. K. Yinda, V. A. Avanzato et al., "Increased small particle aerosol transmission of B.1.1.7 compared with SARS-CoV-2 lineage A in vivo," *Microbiology*, vol. 7, no. 2, pp. 213–223, 2022.

[9] J. Lai, K. K. Coleman, S. H. S. Tai et al., "Exhaled breath aerosol shedding of highly transmissible versus prior severe acute respiratory syndrome coronavirus 2 variants," *Clinical Infectious Diseases*, vol. 76, no. 5, pp. 786–794, 2023.

[10] A. Mikszewski, L. Stabile, G. Buonanno, and L. Morawska, "Increased close proximity airborne transmission of the SARS-CoV-2 Delta variant," *The Science of the Total Environment*, vol. 816, Article ID 151499, 2022.

[11] R. C. K. Law, J. H. Lai, D. J. Edwards, and H. Hou, "COVID-19: research directions for non-clinical aerosol-generating facilities in the built environment," *Buildings*, vol. 11, no. 7, p. 282, 2021.

[12] WHO, "Roadmap to improve and ensure good indoor ventilation in the context of COVID-19," 2021, Accessed June 2023, https://www.who.int/publications/i/item/9789240021280.

[13] J. Lee, S.-H. Park, G.-B. Sung et al., "Effect of air cleaner on reducing concentration of indoor-generated viruses with or without natural ventilation," *Aerosol Science and Technology*, vol. 55, no. 11, pp. 1288–1303, 2021.

[14] K. J. Heo, I. Park, G. Lee et al., "Effects of air purifiers on the spread of simulated respiratory droplet nuclei and virus aggregates," *International Journal of Environmental Research and Public Health*, vol. 18, no. 16, p. 8426, 2021.

[15] T. Lipinski, D. Ahmad, N. Serey, and H. Jouhara, "Review of ventilation strategies to reduce the risk of disease transmission in high occupancy buildings," *International Journal of Thermofluids*, vol. 7, Article ID 100045, 2020.

[16] Y. Qiao, M. Yang, I. A. Marabella et al., "Greater than 3-log reduction in viable coronavirus aerosol concentration in ducted ultraviolet-C (UV–C) systems," *Environmental Science & Technology*, vol. 55, no. 7, pp. 4174–4182, 2021.

[17] E. Eadie, W. Hiwar, L. Fletcher et al., "Far-UVC (222 nm) efficiently inactivates an airborne pathogen in a room-sized chamber," *Scientific Reports*, vol. 12, no. 1, pp. 4373–4373, 2022.

[18] C. Lee, K. H. Park, M. Kim, and Y. B. Kim, "Optimized parameters for effective SARS-CoV-2 inactivation using UVC-LED at 275 nm," *Scientific Reports*, vol. 12, no. 1, Article ID 16664, 2022.

[19] N. Atari, H. Mamane, A. Silberbush, N. Zuckerman, M. Mandelboim, and Y. Gerchman, "Disinfection of SARS-CoV-2 by UV-LED 267 nm: comparing different variants," *Scientific Reports*, vol. 13, no. 1, pp. 8229–8229, 2023.

[20] Y. Feng, J. Zhao, M. Spinolo et al., "Assessing the filtration effectiveness of a portable ultraviolet air cleaner on airborne SARS-CoV-2 laden droplets in a patient room: a numerical study," *Aerosol and Air Quality Research*, vol. 21, no. 5, Article ID 200608, 2021.

[21] H. Dai and B. Zhao, "Reducing airborne infection risk of COVID-19 by locating air cleaners at proper positions indoor: analysis with a simple model," *Building and Environment*, vol. 213, Article ID 108864, 2022.

[22] A. Tobisch, L. Springsklee, L.-F. Schäfer et al., "Reducing indoor particle exposure using mobile air purifiers—experimental and numerical analysis," *AIP Advances*, vol. 11, no. 12, Article ID 125114, 2021.

[23] L. H. Saw, B. F. Leo, C. Y. Lin, N. Mohd Mokhtar, S. H. Md Ali, and M. S. Mohd Nadzir, "The myth of air purifier in mitigating the transmission risk of SARS-CoV-2 virus," *Aerosol and Air Quality Research*, vol. 22, no. 3, Article ID 210213, 2022.

[24] S. Burgmann and U. Janoske, "Transmission and reduction of aerosols in classrooms using air purifier systems," *Physics of Fluids*, vol. 33, no. 3, Article ID 033321, 2021.

[25] J. Curtius, M. Granzin, and J. Schrod, "Testing mobile air purifiers in a school classroom: reducing the airborne transmission risk for SARS-CoV-2," *Aerosol Science and Technology*, vol. 55, no. 5, pp. 586–599, 2021.

[26] D. Dellweg, G. Scheuch, T. Voshaar, and D. Köhler, "Use of portable air purification systems to eliminate aerosol particles from patient rooms," *Aerosol and Air Quality Research*, vol. 22, no. 5, Article ID 210369, 2022.

[27] M. Canpolat, S. Bozkurt, Ç. Şakalar, A. Y. Çoban, D. Karaçaylı, and E. Toker, "Rapid thermal inactivation of aerosolized SARS-CoV-2," *Journal of Virological Methods*, vol. 301, Article ID 114465, 2022.

[28] K. H. Baek, D. Jang, T. Kim et al., "Instant inactivation of aerosolized SARS-CoV-2 by dielectric filter discharge," *PLoS One*, vol. 17, no. 5, Article ID e0268049, 2022.

[29] R. Vuerich, V. Martinelli, S. Vodret et al., "A new laser device for ultra-rapid and sustainable aerosol sterilization," *Environment International*, vol. 164, Article ID 107272, 2022.

[30] Aurabeat Technology Limited, "NSP-W1|AG+ medical grade silver ion antiviral wall mounted air purifier," 2023, https://devices.aurabeattech.com/collections/air-purifiers-for-home/products/nsp-w1-ag-medical-grade-silver-ion-antiviral-wall-mounted-air-purifier.

[31] D.-Y. Chen, N. Khan, B. J. Close et al., "SARS-CoV-2 disrupts proximal elements in the JAK-STAT pathway," *Journal of Virology*, vol. 95, no. 19, Article ID e0086221, 2021.

[32] J. Koch, Z. M. Uckeley, P. Doldan, M. Stanifer, S. Boulant, and P. Lozach, "TMPRSS2 expression dictates the entry route used by SARS-CoV-2 to infect host cells," *The EMBO Journal*, vol. 40, no. 16, Article ID e107821, 2021.

[33] A. Frische, P. T. Brooks, M. Gybel-Brask et al., "Optimization and evaluation of a live virus SARS-CoV-2 neutralization assay," *PLoS One*, vol. 17, no. 7, Article ID e0272298, 2022.

[34] S. F. Sia, L.-M. Yan, A. W. H. Chin et al., "Pathogenesis and transmission of SARS-CoV-2 in golden hamsters," *Nature*, vol. 583, no. 7818, pp. 834–838, 2020.

[35] M. V. Golikov, V. T. Valuev-Elliston, O. A. Smirnova, and A. V. Ivanov, "Physiological media in studies of cell metabolism," *Molecular Biology*, vol. 56, no. 5, pp. 629–637, 2022.

[36] L. Sala-Comorera, L. J. Reynolds, N. A. Martin, J. J. O'Sullivan, W. G. Meijer, and N. F. Fletcher, "Decay of infectious SARS-CoV-2 and surrogates in aquatic environments," *Water Research*, vol. 201, Article ID 117090, 2021.

[37] B. D. Lindenbach, "Measuring HCV infectivity produced in cell culture and in vivo," *Hepatitis C: Methods and Protocols*, vol. 510, pp. 329–336, 2009.

[38] M. Alsved, D. Nygren, S. Thuresson, C.-J. Fraenkel, P. Medstrand, and J. Löndahl, "Size distribution of exhaled aerosol particles containing SARS-CoV-2 RNA," *Infectious Diseases*, vol. 55, no. 2, pp. 158–163, 2023.

[39] R. A. Stern, A. Al-Hemoud, B. Alahmad, and P. Koutrakis, "Levels and particle size distribution of airborne SARS-CoV-2 at a healthcare facility in Kuwait," *The Science of the Total Environment*, vol. 782, Article ID 146799, 2021.

[40] S. Schumacher, A. Caspari, U. Schneiderwind, K. Staack, U. Sager, and C. Asbach, "The drawback of optimizing air cleaner filters for the adsorption of formaldehyde," *Atmosphere*, vol. 15, no. 1, p. 109, 2024.

[41] C. K. Law, J. H. K. Lai, X. D. Ma, and G. N. Sze-To, "Enhancing indoor air quality: examination of formaldehyde adsorption efficiency of portable air cleaner fitted with chemically-treated activated carbon filters," *Building and Environment*, vol. 263, Article ID 111823, 2024.

[42] H. Ueki, M. Ujie, Y. Komori, T. Kato, M. Imai, and Y. Kawaoka, "Effectiveness of HEPA filters at removing infectious SARS-CoV-2 from the air," *mSphere*, vol. 7, no. 4, Article ID e0008622, 2022.

[43] S. Liu, X. Zhao, S. R. Nichols et al., "Evaluation of airborne particle exposure for riding elevators," *Building and Environment*, vol. 207, Article ID 108543, 2022.

[44] T. Dbouk and D. Drikakis, "On airborne virus transmission in elevators and confined spaces," *Physics of Fluids*, vol. 33, no. 1, Article ID 011905, 2021.

[45] J. Gettings, M. Czarnik, E. Morris et al., "Mask use and ventilation improvements to reduce COVID-19 incidence in elementary schools — Georgia, November 16–December 11, 2020," *MMWR. Morbidity and Mortality Weekly Report*, vol. 70, no. 21, pp. 779–784, 2021.

[46] SCMP, "Alarm bells ring in Japan as experts warn of fast-spreading new Covid variant KP.3," 2024, Accessed July 2024, https://www.scmp.com/week-asia/health-environment/article/3270973/alarm-bells-ring-japan-experts-warn-fast-spreading-new-covid-variant-kp3.